

# Formation of $\text{CeSi}_2$ on the Si surface upon high current pulsed Ce-ion implantation

X.Q. Cheng, X.J. Tang, B.X. Liu\*

*Advanced Materials Laboratory, Department of Material Science and Engineering, Tsinghua University, Beijing 100084, China*

Received 2 December 2002; received in revised form 2 June 2003; accepted 2 June 2003

## Abstract

Cerium-ion implantation was conducted to synthesize Ce-disilicide films on silicon wafers, using a metal vapor vacuum arc ion source. The continuous  $\text{CeSi}_2$  films were directly obtained at relatively low temperature with neither external heating nor post-annealing and the surface morphology varied with the variation of the implantation parameters. The formation mechanism of the  $\text{CeSi}_2$  phase is also discussed in terms of the temperature rise caused by ion beam heating and the ion dose in the far-from-equilibrium process of high current pulsed Ce-ion implantation. © 2003 Elsevier B.V. All rights reserved.

**Keywords:** Thin films; Rare earth compounds; Microstructure; X-ray diffraction

## 1. Introduction

Metal silicides have been widely used in very large scale integration (VLSI) technology to form the uniform and thermally stable contacts, interconnects and low-resistivity gates for high-speed and low-power-loss applications [1,2]. Recently rare-earth (RE) metal silicides have attracted considerable attention, because they can form the lowest Schottky barrier height (0.3–0.4 eV) on n-type silicon surface, and because they are also excellent candidate materials of fabricating the advanced infrared detectors [3–5]. Accordingly, various techniques have been extensively developed to synthesize RE metal silicides, such as solid-state reaction (SSR) and ion beam synthesis (IBS) using conventional implanters.

Solid-state reaction was firstly employed to synthesize the RE metal silicides. It was found that the interaction between the RE metals and single crystalline silicon wafers frequently behaves a ‘critical temperature’ phenomenon, i.e., below the critical temperature (320–350 °C), the interaction was sluggish, whereas above the critical temperature, the interaction was explosive [6–8]. As a result, the SSR between the RE metal layer and Si could not be well controlled and the RE metal silicide layers obtained by SSR

were typically dominated with heavy pits, which in turn would have a detrimental effect on the electronic performance [9]. In recent years, IBS technique has also been employed to synthesize the RE metal silicides because of its compatibility with the Si planar technology. In general, the IBS technique using the conventional implanters consists of a high-dose ion implantation at a medium temperature of 350–450 °C and a post-annealing conducted at a temperature as high as 1000 °C. Subsequently, the RE metal silicides could be successfully synthesized under the channeling conditions [10–12]. It is possible to prevent the problem due to high reactivity of RE metals that may degrade the quality of the surface, silicide/Si interface, and silicide layers. Nonetheless, as the conventional implanters could provide weak metal ion current of several pA/cm<sup>2</sup> order, high dose implantation of the order of 10<sup>17</sup>–10<sup>18</sup> ions/cm<sup>2</sup> was time consuming and lasted, at least, for several hours.

It is known that a new ion source, namely the metal vapor vacuum arc (MEVVA) ion source, was invented in the mid-1980s [13], and the source is capable of providing almost all the metal ion species with a very high current density up to 100 μA/cm<sup>2</sup>, which is at least 1–2 orders of magnitude higher than that available in the conventional implanters. Comparatively, the higher dose ion implantation can be completed within less time very effectively at high current metal ion beam. Because of its intense ion current, metal-ion implantation can cause a significant temperature

\* Corresponding author. Fax: +86-10-6277-1160.

E-mail address: dmslxb@tsinghua.edu.cn (B.X. Liu).

rise in the Si surface, resulting in a simultaneous thermal annealing of the Si substrate by ion beam itself. It was therefore possible to synthesize the metal silicides by using high current MEVVA ion source with neither external heating during implantation nor post-annealing. A fast-step technique of the MEVVA ion source has successfully been employed by the authors' group to synthesize the important metal silicides as, such as C54-TiSi<sub>2</sub>,  $\beta$ -FeSi<sub>2</sub>, CoSi<sub>2</sub>, NiSi<sub>2</sub> and ZrSi<sub>2</sub> [14–18]. Currently, the MEVVA ion source works in a pulse mode, i.e., the current density in a pulse is always the same and the increasing of the average current densities is reached by increasing the pulse number within a unit time. The physical process of the metal atoms dynamically launched into the Si lattice in IBS using MEVVA ion source should be obviously different from that of the thermal diffusion and atom migration which emerged in SSR, therefore, the temperature of forming the metal silicide by high current MEVVA ion implantation can probably be considerably lower than that required in SSR [19]. Note that an effective implantation temperature here is defined as the actual temperature rise of the Si wafer caused by the ion beam heating, which could be directly measured, e.g., by a thermal-couple attached on Si surface. We therefore investigate, in the present study, the possibility of directly forming the Ce-disilicide layers on Si wafers by high current Ce-ion implantation and report, in this paper, the experimental observations concerning the formation of the CeSi<sub>2</sub> layers on Si wafers, the effects of ion current as well as dose on the CeSi<sub>2</sub> phase formation and present a brief discussion of the formation mechanism of the CeSi<sub>2</sub> upon MEVVA ion implantation.

## 2. Experimental procedure

The silicon wafers used in this study were n-type Si (100) and Si (111) with a resistivity of 2–4 and 8–10  $\Omega$ -cm. The wafers were cut into 1  $\times$  1-cm<sup>2</sup> samples. The samples were cleaned by a standard chemical procedure and then dipped in a dilute HF solution, followed by a rinse in deionized water. The cleaned samples were then loaded onto a steel-made sample holder in the target chamber of the MEVVA implanter operated at an extract voltage of 45 kV. The vacuum level of the MEVVA implanter was of  $2 \times 10^{-3}$  Pa. During implantation, no deliberate heating was employed for the samples. The samples were implanted with a tilted angle of 7° to minimize channeling effects. As the implantation system has no analysis magnet, the extracted Cerium ions are multiple charged and have been analyzed to consist of 3%Ce<sup>+</sup>, 83%Ce<sup>2+</sup>, 14%Ce<sup>3+</sup>, respectively. The samples were implanted with the current densities varying from 26.4 to 70.4  $\mu$ A/cm<sup>2</sup> to the nominal doses ranging from  $1 \times 10^{17}$  to  $4 \times 10^{17}$  ions/cm<sup>2</sup>. A thermocouple was placed on a non-implanted area of the Si surface to measure the effective temperature rise of the Si substrate during Ce-ion implantation. The MEVVA implanter provided a

pulsed metal-ion beam and the time period of one pulse was 1.2 ms, which was much shorter than the interval (0.3–1.0 s) between two consecutive pulses. Consequently, during high current ion implantation, the temperature rise of the Si substrate increased rapidly upon one pulse shot and then decreased until the next pulse. After a number of pulses, the temperature rise of the Si substrate reached a balanced value, which was actually an average or saturated value during implantation. In high current ion implantation experiments, adjusting the ion current density could vary the temperature rise of the Si substrate and the effect of temperature on the Ce-silicide formation will be discussed later [20]. Since the cathode of the MEVVA ion source was made of Ce with a purity of 99.99 wt%, the purity of the extracted Ce ion beam was considered to be about 99.99 wt%. In order to perform various measurements, at least four samples were prepared for each specific set of implantation parameters.

X-ray diffraction (XRD) was performed to identify the crystalline structure of the formed Ce-silicides after MEVVA ion implantation by a D/max-RB diffractometer operated with a Cu radiation of wavelength 1.5418 Å at 40 kV and 120 mA. A step-scan method was adopted with 0.02° per step and 3 s stopping time at each step. The X-ray beam spot was around 0.5  $\times$  1.0 cm<sup>2</sup>. Rutherford backscattering spectrometry (RBS) was employed to measure the depth profiles of the implanted Ce-ions in the Si wafers with 2.0 MeV He ions at a 165° scattering angle. The ion beam spot was about 2  $\times$  2 mm<sup>2</sup>. A scanning electron microscope (SEM) was used to observe the surface and cross-sectional morphology of the formed Ce-silicide layers on the Si wafers with an acceleration voltage of 10 kV. To obtain reasonable statistics, each measurement was repeated at least twice.

## 3. Results and discussion

### 3.1. Formation of the CeSi<sub>2</sub> phase

We now present the experimental results of CeSi<sub>2</sub> formation upon high current Ce-ion implantation into Si surface using a MEVVA ion source. Since the results obtained in the present study for the Si (100) and Si (111) substrates were similar, for the Si (100) samples, implanted with three different current densities, i.e., 26.4, 52.8 and 70.4  $\mu$ A/cm<sup>2</sup>, to a fixed dose of  $2 \times 10^{17}$  ions/cm<sup>2</sup>, the corresponding XRD patterns of the obtained Ce–Si phase are shown in Fig. 1. From the patterns, one can clearly see that the tetragonal CeSi<sub>2</sub> phase was formed in all of the above cases. The temperature rises of the Si wafers under three different ion current densities of 26.4, 52.8 and 70.4  $\mu$ A/cm<sup>2</sup>, were measured to be of 295, 380 and 430 °C, respectively, with a measurement error of  $\pm 10$  °C. These directly measured temperatures can be considered as the effective formation ones of the Ce-silicide phase under the respective conditions of ion implantation.

We now discuss the effect of ion current density on the formation of the CeSi<sub>2</sub> phase upon a MEVVA ion implantation.

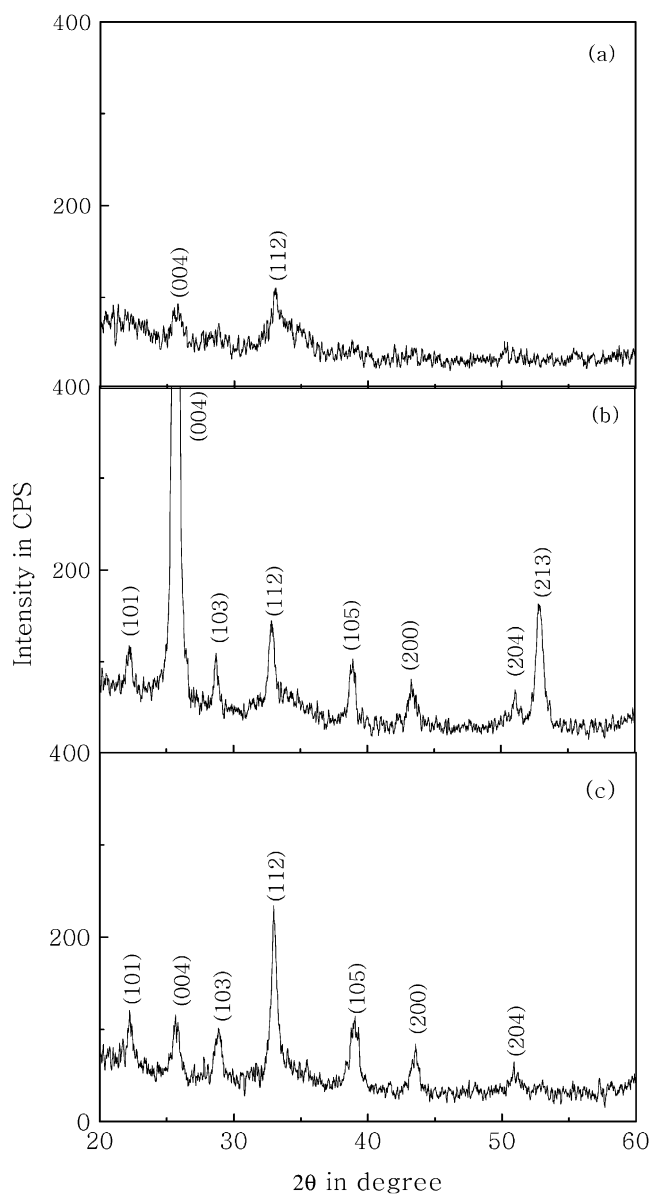


Fig. 1. XRD patterns of Si (100) wafers implanted by Ce-ion with various current densities to a fixed dose of  $2 \times 10^{17}$  ions/cm<sup>2</sup>. (a) 26.4  $\mu\text{A}/\text{cm}^2$ , (b) 52.8  $\mu\text{A}/\text{cm}^2$ , and (c) 70.4  $\mu\text{A}/\text{cm}^2$ .

One sees from Fig. 1(a) that at a current density of 26.4  $\mu\text{A}/\text{cm}^2$ , i.e., at a formation temperature of 295 °C, there are only two weak diffraction peaks (004) and (112) from the CeSi<sub>2</sub> phase. With increasing the ion current density to 52.8  $\mu\text{A}/\text{cm}^2$ , i.e., at the formation temperature of 380 °C, the crystalline structure of the CeSi<sub>2</sub> phase was considerably improved, as shown by the XRD pattern in Fig. 1(b). All the diffraction peaks of CeSi<sub>2</sub> phase obviously appear, although they are very weak except a strong and sharp (004) peak, indicating that an intense texture has emerged. This result shows the possibility of preferential growth of CeSi<sub>2</sub> on Si (100). Further increasing the ion current density up to 70.4  $\mu\text{A}/\text{cm}^2$ , i.e., at the formation temperature of 430 °C,

the diffraction peaks shown in Fig. 1(c) are not stronger than those in the Fig. 1(b), indicating that the crystalline structure was not further improved. Meanwhile, no strong texture appears and it could be not easy to grow up at higher formation temperature. These results indicate that the CeSi<sub>2</sub> phase could be directly obtained at the formation temperature of 380 °C with well-crystallized structure on the Si wafers by single-step ion implantation using the MEVVA ion source.

We also study the effect of ion dose on the CeSi<sub>2</sub> phase formation using the MEVVA ion source. For example, a typical Si (111) sample was implanted by Ce-ion with a fixed ion current density of 52.8  $\mu\text{A}/\text{cm}^2$ , corresponding to a formation temperature of 380 °C, at ion doses ranging from  $1 \times 10^{17}$  to  $4 \times 10^{17}$  ions/cm<sup>2</sup>. At the lowest dose of  $1 \times 10^{17}$  ions/cm<sup>2</sup> in this experiment, the XRD pattern for the Si (111) wafer was obtained as shown in Fig. 2(a). One can see that most diffraction peaks reflected from CeSi<sub>2</sub> phase appear in the spectrum. In Fig. 2(b), with increasing the ion dose up to  $2 \times 10^{17}$  ions/cm<sup>2</sup>, the peaks are a little sharper than those in Fig. 2(a). Further increasing the ion dose up to  $4 \times 10^{17}$  ions/cm<sup>2</sup>, the XRD pattern in Fig. 2(c) shows more diffraction peaks of the CeSi<sub>2</sub> phase with a strong (004) peak. It is therefore concluded that the optimal experimental parameters for synthesizing the continuous CeSi<sub>2</sub> layers on Si (111) wafers by MEVVA ion implantation are an ion current density of about 52.8  $\mu\text{A}/\text{cm}^2$ , corresponding to a formation temperature of approximately 380 °C, and an ion dose around  $2\text{--}4 \times 10^{17}$  ions/cm<sup>2</sup>.

RBS measurement can identify the composition as well as the stoichiometry of the formed CeSi<sub>2</sub> layers. Fig. 3 is a random RBS spectrum of the CeSi<sub>2</sub> layer formed on Si (111) after the implantation with Ce-ion current density of 52.4  $\mu\text{A}/\text{cm}^2$  to a dose of  $4 \times 10^{17}$  ions/cm<sup>2</sup>, corresponding to a formation temperature of 380 °C. One can see that a little plateau signal just behind the Si leading edge appears near the Si surface and the Ce signal is relatively sharp, suggesting that the formed layer is quite thin. As there is no apparent tail at the low-energy edge of the Ce signal, the interface between the formed CeSi<sub>2</sub> layers and the Si substrate might be relatively sharp, which will be further discussed together with the morphology observed from cross-sectional SEM examination.

According to the nominal implantation dose of  $4 \times 10^{17}$  ions/cm<sup>2</sup>, the average range of the Ce-ion deduced from the TRIM program was about 48 nm, which was considered as the thickness of the Ce+Si mixture layer [21]. From the experimental spectrum, the thickness of the formed CeSi<sub>2</sub> was estimated to be about 40 nm, which was much thinner than the former layer [22]. Such a difference could be attributed to the fact that a large portion of the implanted Ce atoms sputtered off from the surface upon interaction of high current Ce-ion with Si substrate. It was estimated that the actual Ce dose retained in the sample is calculated to be about  $8.2 \times 10^{16}$  ions/cm<sup>2</sup>, which is up to the implanted saturation of the Si substrate [23]. Furthermore, the composition profile of the Ce atoms deduced from the spectrum confirmed

to a Gaussian distribution and an average stoichiometry of the formed Ce:Si was determined to be about 1:2.0 with an error of 2.0% at a distance of about 10 nm from the surface, which corresponded quite closely to that of the equilibrium  $\text{CeSi}_2$  phase. It is believed that the irradiation can enhance diffusion of the Ce atoms to a great depth into the Si wafer, resulting in that the Ce concentration at a distance could be small than that in the  $\text{CeSi}_2$  phase.

### 3.2. Surface and cross-sectional morphology of the $\text{CeSi}_2$ layers

In this present study, SEM observations revealed some interesting features of the  $\text{CeSi}_2$  layers obtained on the Si (111) surface by high current pulsed Ce-ion implantation.

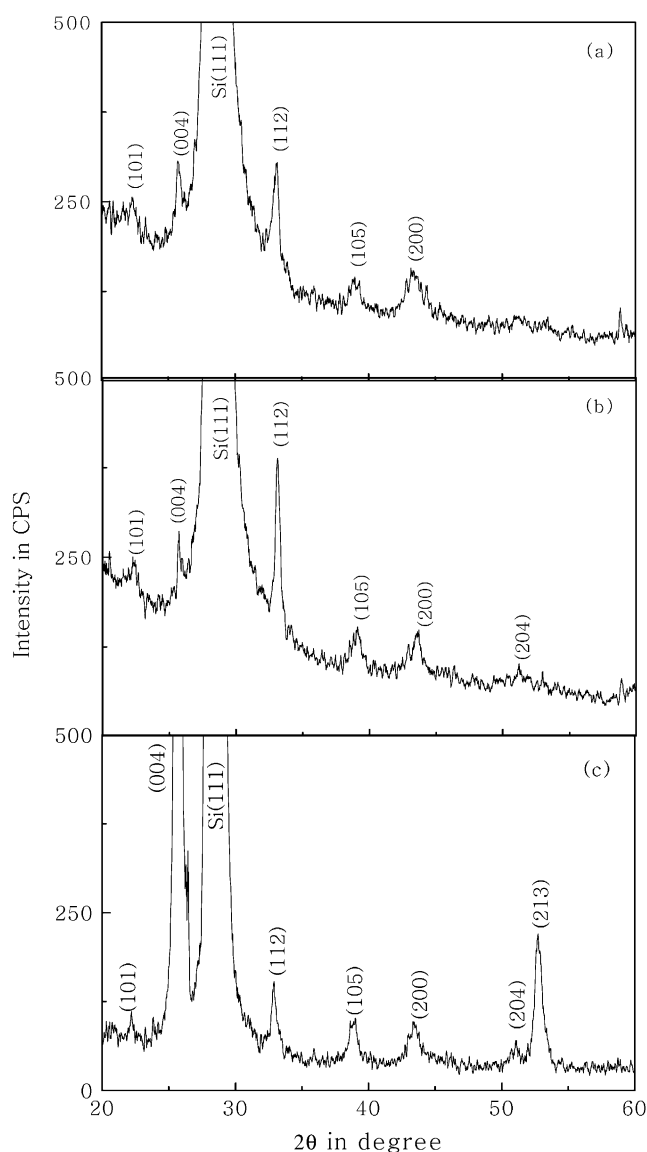


Fig. 2. XRD patterns of Si (111) wafers implanted by Ce-ion with various doses to a fixed current density of  $52.8 \mu\text{A}/\text{cm}^2$ . (a)  $1 \times 10^{17}$  ions/ $\text{cm}^2$ , (b)  $2 \times 10^{17}$  ions/ $\text{cm}^2$ , and (c)  $4 \times 10^{17}$  ions/ $\text{cm}^2$ .

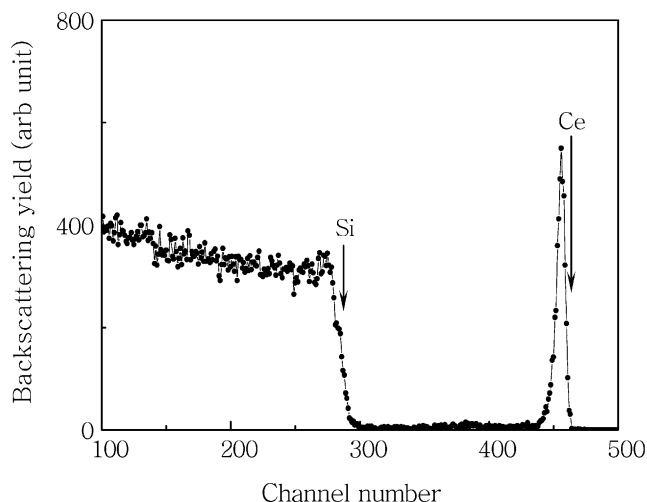


Fig. 3. RBS spectrum of the Si (111) sample with Ce-ion implantation:  $52.8 \mu\text{A}/\text{cm}^2$ ,  $4 \times 10^{17}$  ions/ $\text{cm}^2$ .

Fig. 4(a)–(c) shows a set of SEM morphologies observed from some samples with various effective temperatures during MEVVA ion implantation at the fixed dose of  $2 \times 10^{17}$  ions/ $\text{cm}^2$ . In Fig. 4(a), at the lowest temperature of  $295^\circ\text{C}$ , a network pattern consisting of  $\text{CeSi}_2$  phase (the bright regions) was observed on the Si surface, suggesting that this morphology probably corresponds to an early growth shape of  $\text{CeSi}_2$  grains. When the temperature was increased to  $380^\circ\text{C}$ , the  $\text{CeSi}_2$  grains grew up and embed in the Si substrate, as shown in Fig. 4(b). Further increasing the temperature up to  $430^\circ\text{C}$ , the grain size of the  $\text{CeSi}_2$  layer in Fig. 4(c) is even finer than that in Fig. 4(b), which was because that the higher the temperature the faster the crystals grow and the growing time would decrease when the current density was increased. Consequently, it was a high formation temperature yet with an adequate growing time that resulted in a dense aggregated morphology shown in Fig. 4(c). To study the effect of ion dose, another Si (111) sample was implanted with a current density of  $52.8 \mu\text{A}/\text{cm}^2$  to a dose of  $1 \times 10^{17}$  ions/ $\text{cm}^2$  and the observed morphology is shown in Fig. 4(d). Compared with the case shown in Fig. 4(b), which was twice the dose in Fig. 4(d), one can see that many  $\text{CeSi}_2$  grains did grow larger or upright in a cylindrical shape when the ion dose was increased. It should be noted that the implantation to an additional dose could prolong the reaction time between the Ce ions and the Si substrate, and more Ce atoms was added into the Ce+Si mixture to increase the  $\text{CeSi}_2$  grain size.

In order to examine the continuity of the formed  $\text{CeSi}_2$  layers, the cross-sectional SEM image was observed for the Si (111) sample with a current density of  $52.8 \mu\text{A}/\text{cm}^2$  to a dose of  $2 \times 10^{17}$  ions/ $\text{cm}^2$ . Fig. 5 exhibits the cross-sectional SEM morphology, which clearly shows that the formed  $\text{CeSi}_2$  layer is continuous, and the interface between the  $\text{CeSi}_2$  layers and the Si substrate is relatively sharp.



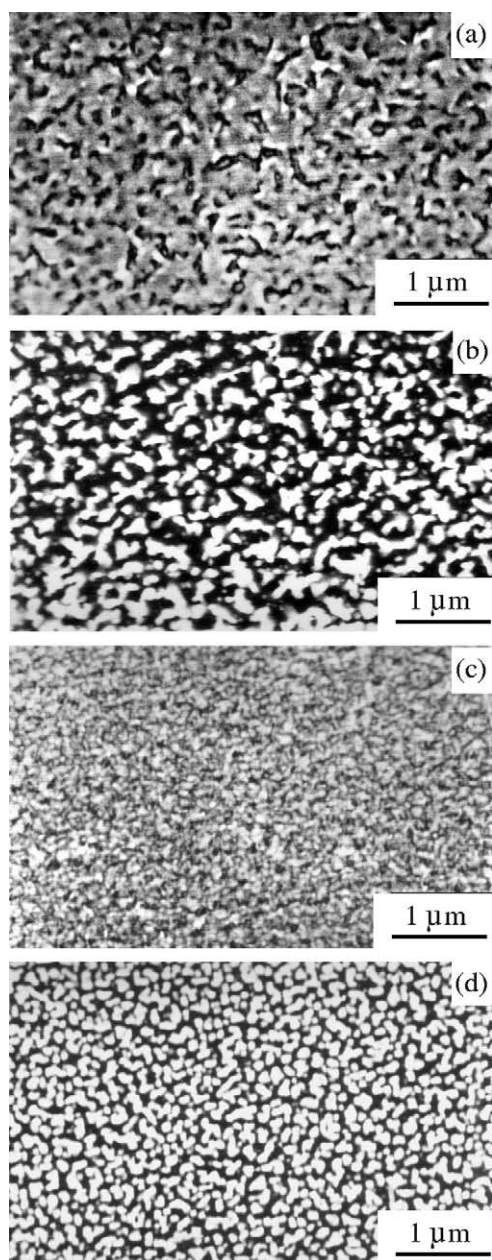


Fig. 4. Surface morphologies of Si (111) wafers implanted by Ce-ions with various conditions. (a)  $26.4 \mu\text{A}/\text{cm}^2$ ,  $2 \times 10^{17}$  ions/ $\text{cm}^2$ , (b)  $52.8 \mu\text{A}/\text{cm}^2$ ,  $2 \times 10^{17}$  ions/ $\text{cm}^2$ , (c)  $70.4 \mu\text{A}/\text{cm}^2$ ,  $2 \times 10^{17}$  ions/ $\text{cm}^2$ , (d)  $52.8 \mu\text{A}/\text{cm}^2$ ,  $1 \times 10^{17}$  ions/ $\text{cm}^2$ .

### 3.3. Formation mechanism of the CeSi<sub>2</sub> layers

We now discuss the formation mechanism of the CeSi<sub>2</sub> phase obtained by MEVVA ion implantation. It is commonly known that the formation of an alloy phase upon energetic ion implantation could be considered in a two-step process. In the first step, atomic collisions are triggered by the irradiating ions and a great number of atoms in the target material together with the irradiating ions are in dynamic motion. During this step, the structure of any desired alloy phase cannot be fixed. The second step named relaxation begins

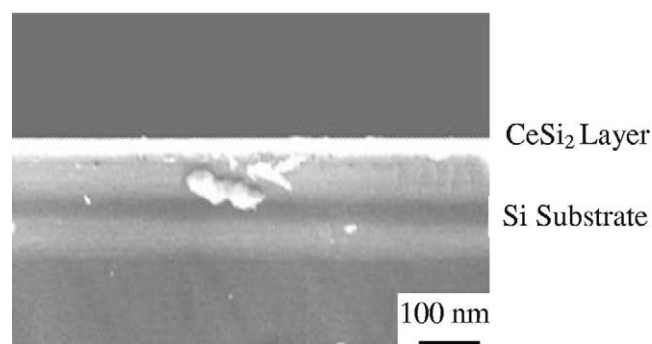


Fig. 5. Cross-sectional SEM image of the formed CeSi<sub>2</sub> layer implanted with Ce-ions with a current density of  $52.8 \mu\text{A}/\text{cm}^2$  to a dose of  $2 \times 10^{17}$  ions/ $\text{cm}^2$ .

at the termination of the atomic collisions and according to the atomic collision theory, it lasts only for extremely short time ( $10^{-10}$  to  $10^{-9}$  s), which allows only simple structured alloy phase to nucleate and grow. As mentioned above, the MEVVA ion source provided a pulsed metal-ion beam. In the present study, the width of the pulse was 1.2 ms and the time interval within two consecutive pulses was 0.3–1.0 s, which was much longer than the relaxation time period after atomic collision.

Accordingly, the formation mechanism of the CeSi<sub>2</sub> phase upon high current Ce-ion implantation was thought to proceed as follows. For simplicity, the process was divided into three steps for each pulsed Ce-ion implantation. Firstly, the high-energy Ce-ions (on the order of keV) were dynamically implanted into the Si lattice to trigger drastic atomic collisions among the Ce and Si atoms. At the termination of Ce-ion implantation and atomic collisions, a highly energetic Ce–Si mixture was obtained and it was most likely in a disordered state. In the second step of relaxation period immediately following the atomic collision, the highly energetic Ce–Si mixture should relax towards equilibrium by some atomic re-arrangement. In the Ce–Si system, the tetragonal CeSi<sub>2</sub> phase is the most stable equilibrium phase having the lowest free energy. Consequently, some crystalline CeSi<sub>2</sub> grains should be formed during the relaxation period. The third step is defined as the time period from the end of the above relaxation to the next implantation pulse and during the third step, the already crystallized CeSi<sub>2</sub> grains should undergo a random walk and organize themselves to form clusters. If the CeSi<sub>2</sub> clusters can grow into a sufficiently large size before the arrival of the next implantation pulse, they are not destroyed completely by the impact of the incoming Ce ions and can remain in the Si surface layer. When the next pulse arrives in, some new CeSi<sub>2</sub> grains could be formed and the growth of the previously retained CeSi<sub>2</sub> clusters could continue to proceed. This growth process can be named intermittent cluster diffusion limited aggregation. The continuation of the above process results in formation of a continuous layer, consisting of CeSi<sub>2</sub> grains that eventually cover the entire Si surface, which was in agreement with the result in Fig. 5.

In Ce-ion implantation, the dynamic process that the energetic Ce ions are implanted into the Si lattice did not require the Si substrate to be at an elevated temperature. However in SSR of deposited metal/Si for the formation of metal silicides, it was necessary to heat the Si substrate to a certain elevated temperature in order to thermally activate the metal atoms to diffuse into the Si substrate. The high current Ce-ion implantation simultaneously caused a significant temperature rise of the Si substrate, which helped in forming the CeSi<sub>2</sub> phase. These two effects made it possible to form the CeSi<sub>2</sub> phase at a considerably lower temperature, which is a process mainly depending on thermal activation and inter-diffusion. In addition, the well-known radiation enhanced diffusion (RED) could also increase the interaction between the Ce atoms and the Si substrates with various temperatures, which could aid in promoting the formation of the CeSi<sub>2</sub> phase as well as in decreasing the effective temperature upon MEVVA ion implantation.

#### 4. Conclusion

We have shown that the equilibrium CeSi<sub>2</sub> phase could directly be synthesized on Si surfaces by a single-step process of high current Ce-ion implantation using MEVVA ion source and that the formed CeSi<sub>2</sub> layers with a well-crystalline structure as well as a smooth surface morphology could be obtained under an optimized condition in high current Ce-ion implantation.

#### Acknowledgements

The financial aids for this study from the National Natural Science Foundation of China, the Ministry of Science and Technology of China (Grant No. G2000067207-1) and the Administration of Tsinghua University are gratefully acknowledged.

#### References

- [1] F.A. d'Avitaya, A. Perio, J.C. Oberlin, Y. Campidelli, J.A. Chroboczek, *Appl. Phys. Lett.* 54 (1989) 2198.
- [2] F.A. d'Avitaya, P.A. Badoz, Y. Campidelli, J.A. Chroboczek, J.Y. Duboz, A. Perio, *Thin Solid Films* 184 (1990) 283.
- [3] J.A. Knapp, S.T. Picraux, *Appl. Phys. Lett.* 48 (1986) 466.
- [4] K.N. Tu, R.D. Thompson, B.Y. Tsaur, *Appl. Phys. Lett.* 38 (1981) 626.
- [5] H. Norde, J. deSousa Pires, F. d'Heurle, F. Pesavento, S. Petersson, P.A. Tove, *Appl. Phys. Lett.* 38 (1981) 865.
- [6] J.E.E. Baglin, F.M. d'Heurle, C.S. Petersson, *Appl. Phys. Lett.* 36 (1980) 594.
- [7] R.D. Thompson, B.Y. Tsaur, K.N. Tu, *Appl. Phys. Lett.* 38 (1981) 535.
- [8] J.E.E. Baglin, F.M. d'Heurle, C.S. Petersson, *J. Appl. Phys.* 52 (1981) 2841.
- [9] S.S. Lau, C.S. Pai, C.S. Wu, T.F. Kuech, B.X. Liu, *Appl. Phys. Lett.* 41 (1982) 77.
- [10] A.E. White, K.T. Short, R.C. Dynes, J.P. Garno, J.M. Gibson, *Appl. Phys. Lett.* 50 (1987) 95.
- [11] M.F. Wu, A. Vantomme, H. Pattyn, G. Langouche, *Appl. Phys. Lett.* 67 (1995) 3886.
- [12] M.F. Wu, A. Vantomme, S. Hogg, H. Pattyn, G. Langouche, *Appl. Phys. Lett.* 72 (1998) 2412.
- [13] I.G. Brown, J.E. Gavin, R.A. MacGill, *Appl. Phys. Lett.* 47 (1985) 358.
- [14] D.H. Zhu, K. Tao, F. Pan, B.X. Liu, *Appl. Phys. Lett.* 62 (1993) 2356.
- [15] B.X. Liu, D.H. Zhu, H.B. Lu, F. Pan, K. Tao, *J. Appl. Phys.* 75 (1994) 3847.
- [16] D.H. Zhu, Y.G. Chen, B.X. Liu, *Nucl. Instrum. Methods B101* (1995) 394.
- [17] K.Y. Gao, B.X. Liu, *Nucl. Instrum. Methods B132* (1997) 68.
- [18] K.Y. Gao, H.N. Zhu, B.X. Liu, *Nucl. Instrum. Methods B140* (1998) 129.
- [19] H.N. Zhu, K.Y. Gao, B.X. Liu, *Phys. Rev. B* 62 (2000) 1647.
- [20] D.H. Zhu, B.X. Liu, *J. Appl. Phys.* 77 (1995) 6257.
- [21] J.F. Ziegler, J.P. Biersack, TRIM (1992) Pergamon Press New York.
- [22] M. Mayer, SIMNRA, V4.0, Max Planck Institute 1997.
- [23] G.W. Reynolds, A.R. Knudson, C.R. Gossett, *Nucl. Instrum. Methods* 182/183 (1981) 179.